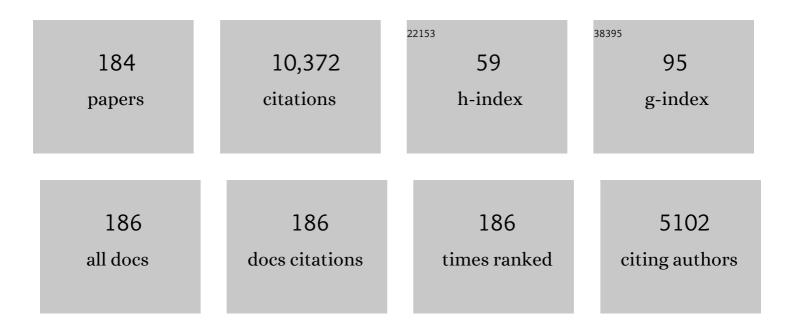
## Guang Ye

## List of Publications by Year in descending order

Source: https://exaly.com/author-pdf/1708784/publications.pdf Version: 2024-02-01



CHANC YE

#	Article	IF	CITATIONS
1	Comparative study of low-cost fluoride removal by layered double hydroxides, geopolymers, softening pellets and struvite. Environmental Technology (United Kingdom), 2022, 43, 4306-4314.	2.2	3
2	A 3D reactive transport model for simulation of the chemical reaction process of ASR at microscale. Cement and Concrete Research, 2022, 151, 106640.	11.0	6
3	A mix design methodology of slag and fly ash-based alkali-activated paste. Cement and Concrete Composites, 2022, 126, 104368.	10.7	55
4	Evaluation of rheology and strength development of alkali-activated slag with different silicates sources. Cement and Concrete Composites, 2022, 128, 104415.	10.7	17
5	A review: Reaction mechanism and strength of slag and fly ash-based alkali-activated materials. Construction and Building Materials, 2022, 326, 126843.	7.2	86
6	M&S highlight: Provis (2014), geopolymers and other alkali activated materials—why, how, and what?. Materials and Structures/Materiaux Et Constructions, 2022, 55, 1.	3.1	0
7	Rheology of alkali-activated slag pastes: New insight from microstructural investigations by cryo-SEM. Cement and Concrete Research, 2022, 157, 106806.	11.0	18
8	Insights in the chemical fundamentals of ASR and the role of calcium in the early stage based on a 3D reactive transport model. Cement and Concrete Research, 2022, 157, 106778.	11.0	6
9	Report of RILEM TC 267-TRM phase 3: validation of the R3 reactivity test across a wide range of materials. Materials and Structures/Materiaux Et Constructions, 2022, 55, .	3.1	32
10	A molecular dynamics study of N–A–S–H gel with various Si/Al ratios. Journal of the American Ceramic Society, 2022, 105, 6462-6474.	3.8	9
11	Thermal deformation and stress of alkali-activated slag concrete under semi-adiabatic condition: Experiments and simulations. Cement and Concrete Research, 2022, 159, 106887.	11.0	6
12	Characterizing the effects of Al(OH)3 and Mg(OH)2 on reaction products and drying shrinkage characteristics of alkali-activated slag. Case Studies in Construction Materials, 2022, 17, e01309.	1.7	1
13	Lattice Boltzmann simulation of the dissolution of slag in alkaline solution using real-shape particles. Cement and Concrete Research, 2021, 140, 106313.	11.0	5
14	GeoMicro3D: A novel numerical model for simulating the reaction process and microstructure formation of alkali-activated slag. Cement and Concrete Research, 2021, 141, 106328.	11.0	5
15	Modelling macroscopic shrinkage of hardened cement paste considering C-S-H densification. Advances in Cement Research, 2021, 33, 257-284.	1.6	1
16	Prediction of the autogenous shrinkage and microcracking of alkali-activated slag and fly ash concrete. Cement and Concrete Composites, 2021, 117, 103913.	10.7	45
17	Determination of specific surface area of irregular aggregate by random sectioning and its comparison with conventional methods. Construction and Building Materials, 2021, 273, 122019.	7.2	15
18	Effect of metakaolin on the autogenous shrinkage of alkali-activated slag-fly ash paste. Construction and Building Materials, 2021, 278, 122397.	7.2	27

#	Article	IF	CITATIONS
19	Role of Curing Conditions and Precursor on the Microstructure and Phase Chemistry of Alkali-Activated Fly Ash and Slag Pastes. Materials, 2021, 14, 1918.	2.9	7
20	A dissolution model of alite coupling surface topography and ions transport under different hydrodynamics conditions at microscale. Cement and Concrete Research, 2021, 142, 106377.	11.0	6
21	3D Microstructure Simulation of Reactive Aggregate in Concrete from 2D Images as the Basis for ASR Simulation. Materials, 2021, 14, 2908.	2.9	7
22	Fracture properties and microstructure formation of hardened alkali-activated slag/fly ash pastes. Cement and Concrete Research, 2021, 144, 106447.	11.0	76
23	Molecular dynamics and experimental study on the adhesion mechanism of polyvinyl alcohol (PVA) fiber in alkali-activated slag/fly ash. Cement and Concrete Research, 2021, 145, 106452.	11.0	43
24	A comparative study on the mechanical properties, autogenous shrinkage and cracking proneness of alkali-activated concrete and ordinary Portland cement concrete. Construction and Building Materials, 2021, 292, 123418.	7.2	25
25	Plastic viscosity of cement mortar with manufactured sand as influenced by geometric features and particle size. Cement and Concrete Composites, 2021, 122, 104163.	10.7	30
26	Early-age properties of alkali-activated slag and glass wool paste. Construction and Building Materials, 2021, 291, 123326.	7.2	14
27	Reactions of self-healing agents and the chemical binding of aggressive ions in sea water: Thermodynamics and kinetics. Cement and Concrete Research, 2021, 145, 106450.	11.0	9
28	New insights into the role of MWCNT in cement hydration. Materials and Structures/Materiaux Et Constructions, 2021, 54, 1.	3.1	1
29	Multi-scale Approach from Atomistic to Macro for Simulation of the Elastic Properties of Cement Paste. Iranian Journal of Science and Technology - Transactions of Civil Engineering, 2020, 44, 861-873.	1.9	6
30	Effects of heat and pressure on hot-pressed geopolymer. Construction and Building Materials, 2020, 231, 117106.	7.2	36
31	Micromechanics-guided development of a slag/fly ash-based strain-hardening geopolymer composite. Cement and Concrete Composites, 2020, 109, 103510.	10.7	57
32	Timeâ€dependent material properties and reinforced beams behavior of two alkaliâ€activated types of concrete. Structural Concrete, 2020, 21, 642-658.	3.1	16
33	New insights into long-term chloride transport in unsaturated cementitious materials: Role of degree of water saturation. Construction and Building Materials, 2020, 238, 117677.	7.2	10
34	Pore size dependent connectivity and ionic transport in saturated cementitious materials. Construction and Building Materials, 2020, 238, 117680.	7.2	31
35	Dependence of unsaturated chloride diffusion on the pore structure in cementitious materials. Cement and Concrete Research, 2020, 127, 105919.	11.0	35
36	Cracking potential of alkali-activated slag and fly ash concrete subjected to restrained autogenous shrinkage. Cement and Concrete Composites, 2020, 114, 103767.	10.7	48

#	Article	IF	CITATIONS
37	THz Fingerprints of Cement-Based Materials. Materials, 2020, 13, 4194.	2.9	9
38	Surface characterization of carbonated recycled concrete fines and its effect on the rheology, hydration and strength development of cement paste. Cement and Concrete Composites, 2020, 114, 103809.	10.7	61
39	A Low-Autogenous-Shrinkage Alkali-Activated Slag and Fly Ash Concrete. Applied Sciences (Switzerland), 2020, 10, 6092.	2.5	7
40	Internal curing of alkali-activated slag-fly ash paste with superabsorbent polymers. Construction and Building Materials, 2020, 263, 120985.	7.2	36
41	Preliminary Interpretation of the Induction Period in Hydration of Sodium Hydroxide/Silicate Activated Slag. Materials, 2020, 13, 4796.	2.9	28
42	Mechanisms of autogenous shrinkage of alkali-activated slag and fly ash pastes. Cement and Concrete Research, 2020, 135, 106107.	11.0	124
43	Internal curing by superabsorbent polymers in alkali-activated slag. Cement and Concrete Research, 2020, 135, 106123.	11.0	71
44	Effect of the Sodium Silicate Modulus and Slag Content on Fresh and Hardened Properties of Alkali-Activated Fly Ash/Slag. Minerals (Basel, Switzerland), 2020, 10, 15.	2.0	45
45	RILEM TC 247-DTA round robin test: carbonation and chloride penetration testing of alkali-activated concretes. Materials and Structures/Materiaux Et Constructions, 2020, 53, 1.	3.1	51
46	Distribution of Lactoferrin Is Related with Dynamics of Neutrophils in Bacterial Infected Mice Intestine. Molecules, 2020, 25, 1496.	3.8	5
47	Evaluating compressive mechanical LDPM parameters based on an upscaled multiscale approach. Construction and Building Materials, 2020, 251, 118912.	7.2	6
48	Modelling microstructural changes of ordinary Portland cement paste at elevated temperature. Advances in Cement Research, 2019, 31, 26-42.	1.6	3
49	Characterization of cogeneration generated Napier grass ash and its potential use as SCMs. Materials and Structures/Materiaux Et Constructions, 2019, 52, 1.	3.1	7
50	RILEM TC 247-DTA round robin test: mix design and reproducibility of compressive strength of alkali-activated concretes. Materials and Structures/Materiaux Et Constructions, 2019, 52, 1.	3.1	53
51	Ink-bottle Effect and Pore Size Distribution of Cementitious Materials Identified by Pressurization–Depressurization Cycling Mercury Intrusion Porosimetry. Materials, 2019, 12, 1454.	2.9	42
52	A Lattice Boltzmann single component model for simulation of the autogenous self-healing caused by further hydration in cementitious material at mesoscale. Cement and Concrete Research, 2019, 123, 105782.	11.0	13
53	Mitigating the autogenous shrinkage of alkali-activated slag by metakaolin. Cement and Concrete Research, 2019, 122, 30-41.	11.0	100
54	Utilization of miscanthus combustion ash as internal curing agent in cement-based materials: Effect on autogenous shrinkage. Construction and Building Materials, 2019, 207, 585-591.	7.2	13

#	Article	IF	CITATIONS
55	Modeling of the chloride diffusivity of ultra-high performance concrete with a multi-scale scheme. Modelling and Simulation in Materials Science and Engineering, 2019, 27, 055002.	2.0	9
56	Chemical deformation of metakaolin based geopolymer. Cement and Concrete Research, 2019, 120, 108-118.	11.0	135
57	Numerical Study on Chloride Ingress in Cement-Based Coating Systems and Service Life Assessment. Journal of Materials in Civil Engineering, 2019, 31, .	2.9	2
58	A review study on encapsulationâ€based selfâ€healing for cementitious materials. Structural Concrete, 2019, 20, 198-212.	3.1	71
59	Investigation on the potential utilization of zeolite as an internal curing agent for autogenous shrinkage mitigation and the effect of modification. Construction and Building Materials, 2019, 198, 669-676.	7.2	34
60	Insights and issues on the correlation between diffusion and microstructure of saturated cement pastes. Cement and Concrete Composites, 2019, 96, 106-117.	10.7	21
61	Effect of curing conditions on the pore solution and carbonation resistance of alkali-activated fly ash and slag pastes. Cement and Concrete Research, 2019, 116, 146-158.	11.0	90
62	A model for predicting the relative chloride diffusion coefficient in unsaturated cementitious materials. Cement and Concrete Research, 2019, 115, 133-144.	11.0	34
63	Pore solution composition of alkali-activated slag/fly ash pastes. Cement and Concrete Research, 2019, 115, 230-250.	11.0	138
64	Influence of moisture condition on chloride diffusion in partially saturated ordinary Portland cement mortar. Materials and Structures/Materiaux Et Constructions, 2018, 51, 1.	3.1	43
65	Effective diffusivity of cement pastes from virtual microstructures: Role of gel porosity and capillary pore percolation. Construction and Building Materials, 2018, 165, 833-845.	7.2	44
66	Rice Husk Ash. RILEM State-of-the-Art Reports, 2018, , 283-302.	0.7	7
67	Carbonation Resistance of Alkali-Activated Slag Under Natural and Accelerated Conditions. Journal of Sustainable Metallurgy, 2018, 4, 33-49.	2.3	41
68	New Test Method for Assessing the Carbonation Front in Alkali-Activated Fly Ash/Slag Pastes. Key Engineering Materials, 2018, 761, 148-151.	0.4	1
69	Development and application of an environmentally friendly ductile alkali-activated composite. Journal of Cleaner Production, 2018, 180, 524-538.	9.3	40
70	Effect of natural carbonation on the pore structure and elastic modulus of the alkali-activated fly ash and slag pastes. Construction and Building Materials, 2018, 161, 687-704.	7.2	70
71	A three-dimensional lattice Boltzmann method based reactive transport model to simulate changes in cement paste microstructure due to calcium leaching. Construction and Building Materials, 2018, 166, 158-170.	7.2	32
72	Reactivity tests for supplementary cementitious materials: RILEM TC 267-TRM phase 1. Materials and Structures/Materiaux Et Constructions, 2018, 51, 1.	3.1	144

#	Article	IF	CITATIONS
73	Setting, Strength, and Autogenous Shrinkage of Alkali-Activated Fly Ash and Slag Pastes: Effect of Slag Content. Materials, 2018, 11, 2121.	2.9	89
74	Numerical Modelling of the Effect of Filler/Matrix Interfacial Strength on the Fracture of Cementitious Composites. Materials, 2018, 11, 1362.	2.9	7
75	CO2 binding capacity of alkali-activated fly ash and slag pastes. Ceramics International, 2018, 44, 19646-19660.	4.8	40
76	Numerical simulation of the initial particle parking structure of cement/geopolymer paste and the dissolution of amorphous silica using real-shape particles. Construction and Building Materials, 2018, 185, 206-219.	7.2	14
77	Microstructure-Based Prediction of the Elastic Behaviour of Hydrating Cement Pastes. Applied Sciences (Switzerland), 2018, 8, 442.	2.5	13
78	Relationship between the Size of the Samples and the Interpretation of the Mercury Intrusion Results of an Artificial Sandstone. Materials, 2018, 11, 201.	2.9	16
79	Pore Structure Characterization of Sodium Hydroxide Activated Slag Using Mercury Intrusion Porosimetry, Nitrogen Adsorption, and Image Analysis. Materials, 2018, 11, 1035.	2.9	29
80	Coupled thermodynamic modelling and experimental study of sodium hydroxide activated slag. Construction and Building Materials, 2018, 188, 262-279.	7.2	51
81	Natural Carbonation of Alkali-Activated Fly Ash and Slag Pastes. , 2018, , 2213-2223.		5
82	Effect of Filler-Hydrates Adhesion Properties on Cement Paste Strength. ACI Materials Journal, 2018, 115, .	0.2	6
83	A Comparative Study on Deflection-Hardening Behavior of Ductile Alkali-Activated Composite. RILEM Bookseries, 2018, , 123-130.	0.4	0
84	Experimental and numerical evaluation of mechanical properties of interface between filler and hydration products. Construction and Building Materials, 2017, 135, 538-549.	7.2	25
85	Examining the "time-zero―of autogenous shrinkage in high/ultra-high performance cement pastes. Cement and Concrete Research, 2017, 97, 107-114.	11.0	91
86	Micro-mechanical properties of alkali-activated fly ash evaluated by nanoindentation. Construction and Building Materials, 2017, 147, 407-416.	7.2	38
87	Effect of fly ash on the pore structure of cement paste under a curing period of 3 years. Construction and Building Materials, 2017, 144, 493-501.	7.2	51
88	Development of porosity of cement paste blended with supplementary cementitious materials after carbonation. Construction and Building Materials, 2017, 145, 52-61.	7.2	123
89	Characterization and comparison of capillary pore structures of digital cement pastes. Materials and Structures/Materiaux Et Constructions, 2017, 50, 1.	3.1	43
90	Waste glass as partial mineral precursor in alkali-activated slag/fly ash system. Cement and Concrete Research, 2017, 102, 29-40.	11.0	161

#	Article	IF	CITATIONS
91	Insights into the mechanisms of nucleation and growth of C–S–H on fillers. Materials and Structures/Materiaux Et Constructions, 2017, 50, 1.	3.1	76
92	Understanding the adhesion mechanisms between C S H and fillers. Cement and Concrete Research, 2017, 100, 275-283.	11.0	90
93	Effect of superabsorbent polymers (SAP) on the freeze–thaw resistance of concrete: results of a RILEM interlaboratory study. Materials and Structures/Materiaux Et Constructions, 2017, 50, 1.	3.1	117
94	Compressive Behavior of Engineered Cementitious Composites under High Strain-Rate Loading. Journal of Materials in Civil Engineering, 2017, 29, .	2.9	37
95	Modeling Framework for Fracture in Multiscale Cement-Based Material Structures. Materials, 2017, 10, 587.	2.9	43
96	Failure Modes in Concrete Repair Systems due to Ongoing Corrosion. Advances in Materials Science and Engineering, 2017, 2017, 1-14.	1.8	5
97	Upscaling Cement Paste Microstructure to Obtain the Fracture, Shear, and Elastic Concrete Mechanical LDPM Parameters. Materials, 2017, 10, 242.	2.9	20
98	A 3D Lattice Modelling Study of Drying Shrinkage Damage in Concrete Repair Systems. Materials, 2016, 9, 575.	2.9	38
99	Effect of Moisture Exchange on Interface Formation in the Repair System Studied by X-ray Absorption. Materials, 2016, 9, 2.	2.9	39
100	Assessment of Structural Feature and Ionic Diffusivity of ITZ in Blended Cementitious Composites. Journal of Advanced Concrete Technology, 2016, 14, 344-353.	1.8	6
101	Numerical Studies of the Effects of Water Capsules on Self-Healing Efficiency and Mechanical Properties in Cementitious Materials. Advances in Materials Science and Engineering, 2016, 2016, 1-10.	1.8	9
102	Studies on the Alkali–Silica Reaction Rim in a Simplified Calcium–Alkali–Silicate System. Materials, 2016, 9, 670.	2.9	5
103	Elastic Modulus of the Alkali-Silica Reaction Rim in a Simplified Calcium-Alkali-Silicate System Determined by Nano-Indentation. Materials, 2016, 9, 787.	2.9	8
104	Modelling the carbonation of cement pastes under a CO2 pressure gradient considering both diffusive and convective transport. Construction and Building Materials, 2016, 114, 333-351.	7.2	79
105	A Review on the Durability of Alkali-Activated Fly Ash/Slag Systems: Advances, Issues, and Perspectives. Industrial & Engineering Chemistry Research, 2016, 55, 5439-5453.	3.7	149
106	Modelling the evolution of microstructure and transport properties of cement pastes under conditions of accelerated leaching. Construction and Building Materials, 2016, 115, 179-192.	7.2	57
107	Diffusivity of saturated ordinary Portland cement-based materials: A critical review of experimental and analytical modelling approaches. Cement and Concrete Research, 2016, 90, 52-72.	11.0	123
108	New insights into autogenous self-healing in cement paste based on nuclear magnetic resonance (NMR) tests. Materials and Structures/Materiaux Et Constructions, 2016, 49, 2509-2524.	3.1	34

#	Article	IF	CITATIONS
109	Anm: a geometrical model for the composite structure of mortar and concrete using real-shape particles. Materials and Structures/Materiaux Et Constructions, 2016, 49, 149-158.	3.1	66
110	Cement hydration and microstructure in concrete repairs with cementitious repair materials. Construction and Building Materials, 2016, 112, 765-772.	7.2	61
111	Self-healing in cementitious materials: Materials, methods and service conditions. Materials and Design, 2016, 92, 499-511.	7.0	237
112	Microstructural characterization of ITZ in blended cement concretes and its relation to transport properties. Cement and Concrete Research, 2016, 79, 243-256.	11.0	183
113	Investigation of the changes in microstructure and transport properties of leached cement pastes accounting for mix composition. Cement and Concrete Research, 2016, 79, 217-234.	11.0	96
114	Physicochemical properties and <i>in vitro</i> mineralization of porous polymethylmethacrylate cement loaded with calcium phosphate particles. Journal of Biomedical Materials Research - Part B Applied Biomaterials, 2015, 103, 548-555.	3.4	16
115	Influence of the Interfacial Transition Zone and Interconnection on Chloride Migration of Portland Cement Mortar. Journal of Advanced Concrete Technology, 2015, 13, 169-177.	1.8	24
116	Effect of limestone fillers on microstructure and permeability due to carbonation of cement pastes under controlled CO 2 pressure conditions. Construction and Building Materials, 2015, 82, 376-390.	7.2	105
117	Ultrahigh performance concrete-properties, applications and perspectives. Science China Technological Sciences, 2015, 58, 587-599.	4.0	92
118	Self-healing of cracks in cement paste affected by additional Ca <sup>2+</sup> ions in the healing agent. Journal of Intelligent Material Systems and Structures, 2015, 26, 309-320.	2.5	48
119	A review of the chloride transport properties of cracked concrete: experiments and simulations. Journal of Zhejiang University: Science A, 2015, 16, 81-92.	2.4	30
120	Combined experimental and numerical study of fracture behaviour of cement paste at the microlevel. Cement and Concrete Research, 2015, 73, 123-135.	11.0	61
121	The shrinkage of alkali activated fly ash. Cement and Concrete Research, 2015, 68, 75-82.	11.0	173
122	Micromechanical Study of the Interface Properties in Concrete Repair Systems. Journal of Advanced Concrete Technology, 2014, 12, 320-339.	1.8	40
123	The ITZ microstructure, thickness and porosity in blended cementitious composite: Effects of curing age, water to binder ratio and aggregate content. Composites Part B: Engineering, 2014, 60, 1-13.	12.0	153
124	Effect of blast furnace slag on self-healing of microcracks in cementitious materials. Cement and Concrete Research, 2014, 60, 68-82.	11.0	148
125	Multiscale lattice Boltzmann-finite element modelling of chloride diffusivity in cementitious materials. Part II: Simulation results and validation. Mechanics Research Communications, 2014, 58, 64-72.	1.8	33
126	Effect of internal curing by using superabsorbent polymers (SAP) on autogenous shrinkage and other properties of a high-performance fine-grained concrete: results of a RILEM round-robin test. Materials and Structures/Materiaux Et Constructions, 2014, 47, 541-562.	3.1	175

#	Article	IF	CITATIONS
127	Influence of particle size on the early hydration of slag particle activated by Ca(OH)2 solution. Construction and Building Materials, 2014, 52, 488-493.	7.2	18
128	Feasibility of self-healing in cementitious materials – By using capsules or a vascular system?. Construction and Building Materials, 2014, 63, 108-118.	7.2	71
129	Fractal and multifractal analysis on pore structure in cement paste. Construction and Building Materials, 2014, 69, 253-261.	7.2	74
130	Tailoring strain-hardening cementitious composite repair systems through numerical experimentation. Cement and Concrete Composites, 2014, 53, 200-213.	10.7	41
131	A versatile pore-scale multicomponent reactive transport approach based on lattice Boltzmann method: Application to portlandite dissolution. Physics and Chemistry of the Earth, 2014, 70-71, 127-137.	2.9	33
132	Multiscale lattice Boltzmann-finite element modelling of chloride diffusivity in cementitious materials. Part I: Algorithms and implementation. Mechanics Research Communications, 2014, 58, 53-63.	1.8	38
133	Microstructural and permeability changes due to accelerated Ca leaching in ammonium nitrate solution. , 2014, , 431-438.		2
134	Quantitative analysis of phase transition of heated Portland cement paste. Journal of Thermal Analysis and Calorimetry, 2013, 112, 629-636.	3.6	36
135	Determination of water permeability of cementitious materials using a controlled constant flow method. Construction and Building Materials, 2013, 47, 1488-1496.	7.2	69
136	Simulation of the microstructure formation in hardening self-compacting cement paste containing limestone powder as filler via computer-based model. Materials and Structures/Materiaux Et Constructions, 2013, 46, 1861-1879.	3.1	5
137	Characterization and quantification of self-healing behaviors of microcracks due to further hydration in cement paste. Cement and Concrete Research, 2013, 52, 71-81.	11.0	198
138	A microscopic study on ternary blended cement based composites. Construction and Building Materials, 2013, 46, 28-38.	7.2	13
139	Micro- and meso-scale pore structure in mortar in relation to aggregate content. Cement and Concrete Research, 2013, 52, 149-160.	11.0	61
140	Microstructure-based modeling of permeability of cementitious materials using multiple-relaxation-time lattice Boltzmann method. Computational Materials Science, 2013, 68, 142-151.	3.0	56
141	New perspective of service life prediction of fly ash concrete. Construction and Building Materials, 2013, 48, 764-771.	7.2	26
142	Characterization of ITZ in ternary blended cementitious composites: Experiment and simulation. Construction and Building Materials, 2013, 41, 742-750.	7.2	73
143	The pore structure of cement paste blended with fly ash. Construction and Building Materials, 2013, 45, 30-35.	7.2	149
144	Porosity characterization of ITZ in cementitious composites: Concentric expansion and overflow criterion. Construction and Building Materials, 2013, 38, 1051-1057.	7.2	90

#	Article	IF	CITATIONS
145	Investigation of the structure of heated Portland cement paste by using various techniques. Construction and Building Materials, 2013, 38, 1040-1050.	7.2	86
146	Microstructure-based modeling of the diffusivity of cement paste with micro-cracks. Construction and Building Materials, 2013, 38, 1107-1116.	7.2	40
147	The pore structure and permeability of alkali activated fly ash. Fuel, 2013, 104, 771-780.	6.4	230
148	Concrete in Engineered Barriers for Radioactive Waste Disposal Facilities: Phenomenological Study and Assessment of Long Term Performance. , 2013, , .		4
149	Microstructure of Cement Paste Blended with Micronized Sand (MS). Building Pathology and Rehabilitation, 2013, , 61-84.	0.2	2
150	Dehydration kinetics of Portland cement paste at high temperature. Journal of Thermal Analysis and Calorimetry, 2012, 110, 153-158.	3.6	134
151	Modeling of ionic diffusivity in non-saturated cement-based materials using lattice Boltzmann method. Cement and Concrete Research, 2012, 42, 1524-1533.	11.0	71
152	Experimental study on alinite ecocement clinker preparation from municipal solid waste incineration fly ash. Materials and Structures/Materiaux Et Constructions, 2012, 45, 1145-1153.	3.1	13
153	Preparation of alinite cement from municipal solid waste incineration fly ash. Cement and Concrete Composites, 2012, 34, 322-327.	10.7	58
154	Improved fiber distribution and mechanical properties of engineered cementitious composites by adjusting the mixing sequence. Cement and Concrete Composites, 2012, 34, 342-348.	10.7	155
155	Simulation of self-healing by further hydration in cementitious materials. Cement and Concrete Composites, 2012, 34, 460-467.	10.7	103
156	Computational investigation on mass diffusivity in Portland cement paste based on X-ray computed microtomography (μCT) image. Construction and Building Materials, 2012, 27, 472-481.	7.2	123
157	Estimation of the ionic diffusivity of virtual cement paste by random walk algorithm. Construction and Building Materials, 2012, 28, 405-413.	7.2	65
158	Microstructure Analysis of Heated Portland Cement Paste. Procedia Engineering, 2011, 14, 830-836.	1.2	17
159	Hydration and microstructure of ultra high performance concrete incorporating rice husk ash. Cement and Concrete Research, 2011, 41, 1104-1111.	11.0	288
160	Modeling of the internal damage of saturated cement paste due to ice crystallization pressure during freezing. Cement and Concrete Composites, 2011, 33, 562-571.	10.7	85
161	Microstructure-based modeling of water diffusivity in cement paste. Construction and Building Materials, 2011, 25, 2046-2052.	7.2	40
162	The study of using rice husk ash to produce ultra high performance concrete. Construction and Building Materials, 2011, 25, 2030-2035.	7.2	265

#	Article	IF	CITATIONS
163	Development of engineered cementitious composites with limestone powder and blast furnace slag. Materials and Structures/Materiaux Et Constructions, 2010, 43, 803-814.	3.1	177
164	Modelling of time dependency of chloride diffusion coefficient in cement paste. Journal Wuhan University of Technology, Materials Science Edition, 2010, 25, 687-691.	1.0	8
165	Numerical simulation on moisture transport in cracked cement-based materials in view of self-healing of crack. Journal Wuhan University of Technology, Materials Science Edition, 2010, 25, 1077-1081.	1.0	8
166	Characterization of pore structure in cement-based materials using pressurization–depressurization cycling mercury intrusion porosimetry (PDC-MIP). Cement and Concrete Research, 2010, 40, 1120-1128.	11.0	189
167	Early-Age Heat Evolution and Pore Structure of Portland Cement Blended with Blast Furnace Slag, Fly Ash or Limestone Powder. Key Engineering Materials, 2009, 405-406, 242-246.	0.4	2
168	Self-healing behavior of strain hardening cementitious composites incorporating local waste materials. Cement and Concrete Composites, 2009, 31, 613-621.	10.7	243
169	On the mechanism of polypropylene fibres in preventing fire spalling in self-compacting and high-performance cement paste. Cement and Concrete Research, 2008, 38, 487-499.	11.0	162
170	Modelling of stresses and strains in bonded concrete overlays subjected to differential volume changes. Theoretical and Applied Fracture Mechanics, 2008, 49, 199-205.	4.7	30
171	Modelling the performance of ECC repair systems under differential volume changes. , 2008, , 363-364.		1
172	Simulation of Failure in Hydrating Cement Particles Systems. Key Engineering Materials, 2007, 348-349, 737-740.	0.4	1
173	Phase distribution and microstructural changes of self-compacting cement paste at elevated temperature. Cement and Concrete Research, 2007, 37, 978-987.	11.0	98
174	Influence of limestone powder used as filler in SCC on hydration and microstructure of cement pastes. Cement and Concrete Composites, 2007, 29, 94-102.	10.7	300
175	Influence of Boundary Conditions on Pore Percolation in Model Cement Paste. Key Engineering Materials, 2006, 302-303, 486-492.	0.4	29
176	Percolation of capillary pores in hardening cement pastes. Cement and Concrete Research, 2005, 35, 167-176.	11.0	130
177	Study on the development of the microstructure in cement-based materials by means of numerical simulation and ultrasonic pulse velocity measurement. Cement and Concrete Composites, 2004, 26, 491-497.	10.7	124
178	Three-dimensional microstructure analysis of numerically simulated cementitious materials. Cement and Concrete Research, 2003, 33, 215-222.	11.0	104
179	3D Lattice Fracture Model: Theory and Computer Implementation. Key Engineering Materials, 0, 452-453, 69-72.	0.4	4
180	3D Lattice Fracture Model: Application to Cement Paste at Microscale. Key Engineering Materials, 0, 452-453, 65-68.	0.4	5

#	Article	IF	CITATIONS
181	Effect of Limestone Fillers on Ca-Leaching and Carbonation of Cement Pastes. Key Engineering Materials, 0, 711, 269-276.	0.4	4
182	Shrinkage Behavior of Alkali-Activated Slag Cement Pastes. Key Engineering Materials, 0, 761, 45-48.	0.4	15
183	Coupling of Hydration and Fracture Models: Failure Mechanisms in Hydrating Cement Particle Systems. , 0, , 563-571.		2
184	Alkali-Activated Materials as Alternative Binders for Structural Concrete: Opportunities and Challenges. , 0, , .		0